A PROBABILISTIC WARNING SYSTEM FOR SAFE CURVE NEGOTIATION

Guillaume Rey
David Clair
Michel Fogli
Laboratoire de Mécanique et Ingénierie (LaMI)
France
Frédéric Bernardin
Laboratoire Régional des Ponts et Chaussées (LRPC)
France
Paper Number 09-0141

ABSTRACT

While empirical evidence shows the main effects of the driving style (principally speed choices) on safety, this study aims to quantify the influent parameters and their interactions upon the roadway departure risk. A previous work [1] using a sensitivity analysis concludes that speed, lateral position on the pavement, total embedded mass and mass center position are the relevant parameters. They constitute what is called initial conditions in the following. Probabilistic methods for the risk assessment are proposed to deal with uncertainties arising from the road infrastructure, the vehicle characteristics and the driver behaviour. Those methods originally developed in the field of structural reliability reveal promising interest in the road safety question as they allow the direct computation of a risk index, not provided by a deterministic modeling. This approach involves both measurements on real traffic by static video sensors and simulations from a specifically developed model. A set of 400 experimental trajectories is used to define mean trajectories among different classes of drivers for one turn, and simulated ones are necessary for the reliability index calculation. The result of this study is a surface response of the roadway departure probability against initial speed and lateral position on the pavement. This work will lead to the development of a warning system within the French national project SARI. Envisaged alert procedures are warning light flashes inviting the driver to modify his trajectory if the risk index calculated at the entrance of the curve indicates a dangerous situation. Difficulty for short-term implementation comes from the statistical characterization of the initial conditions (i.e. mean value and standard deviation), especially for mass and mass centre position measurement device on standard vehicles.

INTRODUCTION

The 2006 French road safety figures confirm that a large majority (75%) of casualties occurs on secondary roads, which only cover 52% of the traffic. Among these accidents, the most frequent type is Single Vehicle Roadway Departure (SVRD) during cornering. The aim of the present study, conducted through the French national project SARI, is to develop a SVRD warning system that could equip dangerous turns.

SVRD prevention system are currently an active field of research [2-6] since it is a natural evolution of the Electronic Stability Program (ESP) and the lane departure prevention systems that are at the state of commercialization. Compared to these studies, the originality of the method presented here relies on two major points. First, SRVD prevention systems are generally based on forward looking camera, thus requiring specific equipment embedded in the car. This is an obstacle for a mass implementation of the system. On the contrary, the risk assessment process proposed here is thought to work with in-pavement integrated measurement devices for acquiring initial conditions at the curve entrance. Second, the specific vehicle dynamics model developed ensures that the simulated trajectories are physically realizable in comparison with trajectories geometrically defined. This also allows to introduce the inherent hazard contained in the driver's action, the road infrastructure and the vehicle by modeling the real physical parameters by random variables. Hence the statistical characterization of these variables is facilitated, compared to other studies [7] where non-physical parameters are used to perturb the system.

Expected results of this study is a roadway departure risk evaluation based on a flexible list of criteria, thus more general than Curve Speed Warning or Time to Line Crossing usually used in this context. Risk indicator evolution is here studied as a function of speed and initial lateral position at the entrance of the curve.

Approach

This study is based on structural reliability methods [8] that directly provide the computation of a risk

index. This calculation is based on simulated trajectories that reflect the possible trajectories that could be realized by the driver. These simulations are performed using a vehicle dynamics model in which uncertainties are introduced via random variables. These random variables have been chosen in a previous study [1] using a sensitivity analysis [9,10]. They represent the uncertainties arising from the driver, the vehicle and the road infrastructure. The risk evaluation process from the vehicle arrival to the alarm triggering decision is made up of three steps:

- Several position and speed measurements points placed before the curve provide information on the driver behaviour at the turn entrance. Vehicle characteristics are set to the adequate values into the dynamic model. This data set constitutes what is called next "initial conditions".
- A reference trajectory is associated to these initial conditions. This trajectory reflects the behaviour of a standard driver. The definition of this trajectory using real traffic measurements is the object of the second part of this study.
- Finally, risk assessment consists in quantifying the chances that the simulated trajectories violate the safety criteria.

VEHICLE DYNAMICS MODELING

In this first part, the vehicle dynamics model specifically developed for this application is briefly detailed, then safety criteria are chosen to distinguish between a safe and a dangerous trajectory, and finally some random variables are introduced in the model to take into account the inherent variability of the triptych *driver-vehicle-road infrastructure*.

Deterministic modeling

The basis of the vehicle dynamics model is the 3 degrees of freedom *yaw-slip-roll* model [11,12] chosen for its fast computation and satisfying accuracy. Positioning is made using the orientation angle θ and the slip angle α (see Figure 1). The driver imposes the vehicle path through the steering angle β and the vehicle speed V. The roll angle is parameterized by the angle φ.

Compared to the classical *yaw-slip-roll* model, improvements are made concerning three points:

Tire forces - Governing the tire/ground interaction, the evolution of the lateral force F_{Yi} against the influent parameters requires a careful modeling. The tire slip angle δ_i non-linear effect is modeled using the *magic formula* [13]. The normal

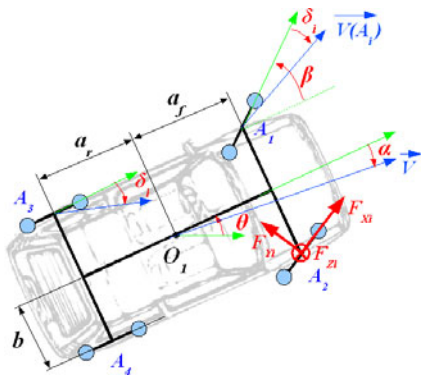

Figure 1. Scheme of the vehicle model.

force F_{Zi} influences the cornering stiffness according to the *similarity method* [14]. The last considered effect concerns the interaction between the longitudinal force F_{Xi} and the lateral force F_{Yi}, where a factor $\phi_{xi} \leq 1$ ensures that the in plane resultant force remains into the friction circle, defined by the friction coefficient μ.

Suspensions - Springs, dampers and a front anti-roll bar are considered for the calculation of the roll angle φ. Pitch and heave are neglected. For a better agreement with a complete simulator [15] in hard cornering situations, initial toe angles and roll steer phenomenon [12] are taken into account.

Time dependent input - To handle with realistic cases, variable driver commands and road infrastructure characteristics need to be simulated. Hence braking situation while cornering, as well as measured banking and slope angles can be implemented in the model.

The equation of motion is now expressed using the state vector $\boldsymbol{x_s} = (\alpha, \dot{\theta}, \dot{\varphi}, \varphi, V)^T$, the command vector $\boldsymbol{u} = (\beta, F_{X1}, \ldots, F_{X4})^T$ and the external loads. It is of the form:

$$\begin{cases} \dot{\boldsymbol{x}}_s(t) = A^{-1}(\boldsymbol{x}_s(t))F(\boldsymbol{x}_s(t), \boldsymbol{u}(t)), t > 0 \\ \boldsymbol{x}_s(0) = \boldsymbol{x}_{s0} \end{cases} \quad (1)$$

where the matrix A and the function F are calculated with the laws of motion. Trajectories can be computed once given the initial conditions $\boldsymbol{x_{s0}}$ and driver commands $\boldsymbol{u}$. The resolution of the model is made using the second order Runge-Kutta method.

Safety criteria

Safety criteria are used to classify the safe and unsafe trajectories. Two criteria are generally used

when dealing with road safety, and especially lane departure and rollover prevention. Curve Speed Warning (CSW) defines a reference speed for which the slip limit is reached for the upcoming curve. Time to Line Crossing (TLC) computes the remaining time before the lane boundary is reached, under different assumptions on the future trajectory (e.g. straight line or circular trajectory). Although showing promising results on field testing [2] in deterministic studies, basic criteria are preferred here to simplify the interpretation of these first results. Anyway, the criteria list may be modified later without any concern on the proposed methodology.

The safety criteria used in this paper are based on the lateral position d (algebraic distance from the middle of the lane) and the lateral acceleration a_y. These two control variables are functions of the state vector $\boldsymbol{x}_s$:

$$d(t) = \eta_1(\boldsymbol{x}_s(t)) \tag{2}$$

$$a_y(t) = \eta_2(\boldsymbol{x}_s(t)) \tag{3}$$

Thresholds $\overline{d}$ and $\overline{a_y}$ on the control variables define the safety criteria (i.e. the trajectory is considered as dangerous if one criterion is violated). These criteria are defined by:

$$\overline{d} - \sup_{t\in[0,T]} |d(t)| > 0 \tag{4}$$

$$\overline{a_y} - \sup_{t\in[0,T]} |a_y(t)| > 0 \tag{5}$$

where T is the total observation time. For this application, $\overline{d}$ equals the half difference between the lane width and the vehicle width and $\overline{a_y}$ is chosen equal to 3 m.s^{-2} so that a margin is kept with respect to the vehicle handling limits.

Stochastic modeling

Among all the model parameters (linked to the triptych *driver-vehicle-road infrastructure*) some present a marked random variability. Therefore it is crucial for the credibility of the approach to take into account this reality via a suited stochastic modeling. In order to reduce the calculation time and improve the model robustness, the number of random variables introduced in the model has to be optimized. This study has been made previously [1] using a global sensitivity analysis based on Sobol' indices [10]. It has been concluded that the choice of the total embedded mass M, the centre of mass position a_r, the initial lateral position D_0 and an additive speed perturbation V_0 as random parameters guarantees an efficient representativity of the uncertainties propagation through the mechanical model. These parameters are gathered in the vector $\boldsymbol{x} = (M, a_r, D_0, V_0)^T$, and this vector is modelled as a $\Re^4$-valued random variable denoted $\boldsymbol{X} = (X_1, \ldots, X_4)^T$, for which the following hypotheses are made:

(H1) its components $X_1, \ldots, X_4$ are mutually independent ;

(H2) each of its components follows a truncated Gaussian distribution, which characteristics are given in Table 1 ;

(H3) the support of the truncated Gaussian distribution is chosen of the form mean ±3 standard deviations.

Since in equation (1) the functions A and F and the initial condition $\boldsymbol{x}_{s0}$ depend on $\boldsymbol{x}$, when this deterministic vector is considered as a random vector $\boldsymbol{X}$, A, F and $\boldsymbol{x}_{s0}$ become random, and consequently the state vector function $\boldsymbol{x}_s(t)$ becomes a random process $\boldsymbol{X}_s(t)$ governed by the equation :

$$\begin{cases} \dot{\boldsymbol{X}}_s(t) = A^{-1}(\boldsymbol{X}_s(t))F(\boldsymbol{X}_s(t), \boldsymbol{u}(t)), t > 0 \\ \boldsymbol{X}_s(0) = \boldsymbol{X}_{s0} \end{cases} \tag{6}$$

in which the driver command $\boldsymbol{u}$ is kept deterministic and $\boldsymbol{X}_{s0}$ is a $\Re^5$-valued random variable depending on $\boldsymbol{X}$.

In this random context, the control variables d and a_y given by equations (2) and (3) are random processes D and A_y such that, $\forall t \in \Re_+$:

$$D(t) = \eta_1(\boldsymbol{X}_s(t)) \tag{7}$$

$$A_y(t) = \eta_2(\boldsymbol{X}_s(t)) \tag{8}$$

The aim of this study is to quantify the risk for the safety criteria to be violated. For that, once the initial conditions of the arriving vehicles are measured, a reference trajectory (which defines the driver commands) must be associated to begin the risk evaluation process. This is the object of the next section.

x	Parameter	X	Unit	Mean	Standard deviation	Truncation interval
M	Total embedded mass	X_1	kg	1610	16	[1562;1658]
a_r	Rear axle location	X_2	m	1.532	0.01	[1.502;1.562]
D_0	Position perturbation	X_3	m	0	0.2	[-0.6;0.6]
V_0	Velocity perturbation	X_4	km.h^{-1}	0	0.1	[-0.3;0.3]

Table 1. Statistical characteristics of the random variables.

REFERENCE TRAJECTORY

The reference trajectory is defined here as the trajectory that a mean driver would have realized if he has entered the curve with the given initial conditions $\boldsymbol{X}$. Therefore a theoretical definition of this trajectory is hardly realizable as it depends on a lot of factors (driving style, visibility conditions, …). Even if studies defining a driver model are topical [16-19], choice has been made to deduce the reference trajectory from real traffic measurements in order to get more realistic results.

Traffic measurement

This work has been carried out by Goyat and al. [20] in an other task of the SARI project, which consisted in the development of a portable trajectory measurement device. The measurement is based on cameras and telemeter. Images are then processed to estimate the vehicle position and velocity (Figure 2).

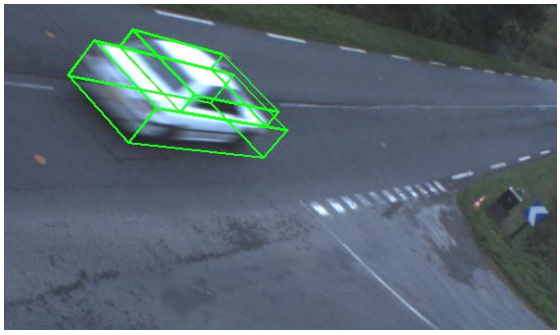

Figure 2. Image processing for position estimation.

This system has been deployed for measurements during two days on a French secondary road, and led to the construction of a 400 trajectory database. The figures 3 and 4 show the tendency of the drivers' behaviours during the curve. It can be noticed that at the entry of the right curve (on the right of the figure), drivers are mostly at the outside of the lane. It can be explained by the fact that the studied curve is preceded by a slight bend on the left and it appears that drivers tend to cut this curve. This is an example of the effects that are hardly predictable in driver models. The exit of the curve is followed by a straight line, and trajectories use the entire width of the lane with a mode nearly in the middle.

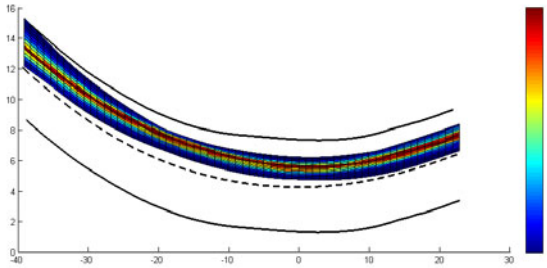

Figure 3. Density field of vehicle passage, over the 400 experimental trajectories (not to scale).

Figure 4 shows the cumulative repartition of the trajectory percentage as a function of the speed measured at the entrance, in the middle or at the exit of the curve. At the entrance of the curve, the V85 indicator (speed for which 85% of the traffic is driving slower) is 66km/h. It is far below the effective speed limit for this turn (90 km/h). So this curve negotiation requires from the driver a quick estimation of the speed that he estimates comfortable and safe, what can lead to dangerous situations. This makes this turn to be an interesting application for this study.

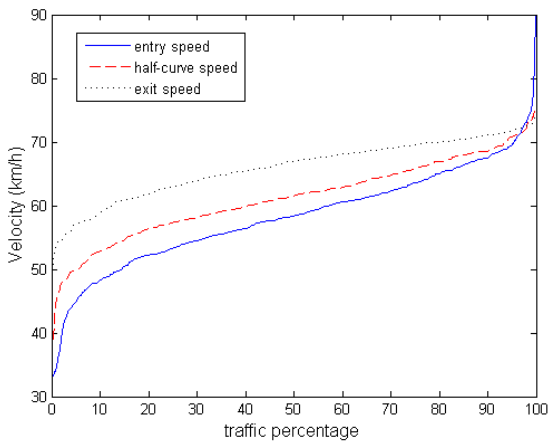

Figure 4. Measured velocity in traffic, for different position in the curve.

Driver classes

The 400 experimental trajectories are separated in different classes of driving style, so that a reference trajectory per class can be identified. As the choice of the reference trajectory must be done upon the initial conditions values, the classes definition must be made on variables measurable at the entrance of the curve. Owing to the measurement device used, these variables are restricted to the initial lateral position y_e and the initial speed v_e.

The first step of this analysis is to look for a correlation between y_e and v_e. The intuitive belief being that a driver entering at a higher speed would tend to cut the curve, implying an exterior lane positioning. Figure 5 shows the scattered plot of v_e in function of y_e. Indeed, the widespread shape of the graph does not indicate any correlation between speed and position.

Hence it has been chosen to separate the drivers classes only according to their initial lateral position y_e. Four classes of 50 cm width are created, as shown by the different colours in Figure 5. In each of these classes, the reference

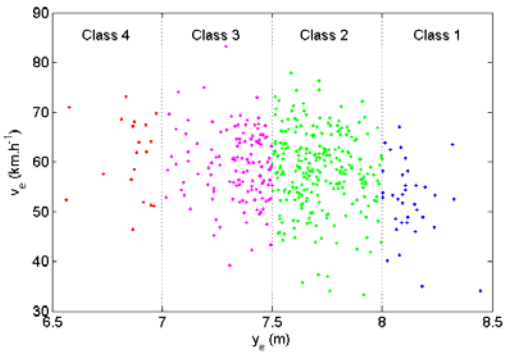

Figure 5. Scattered plot of initial speed as a function of initial lateral position.

trajectory is defined by the mean of the experimental trajectories. Results are presented on Figure 6. Classes are numbered from the interior (class 1) to the exterior (class 4).

Command computation

Once the reference trajectory is defined, the corresponding driver commands (steer angle and associated speed) must be computed to start the risk estimation process. This is done by inverting the vehicle dynamics model at each of the *N* steps of the simulation, thus resolving for all $n \in [1, N]$:

$$d_{lat}(\beta_n) = 0 \qquad (9)$$

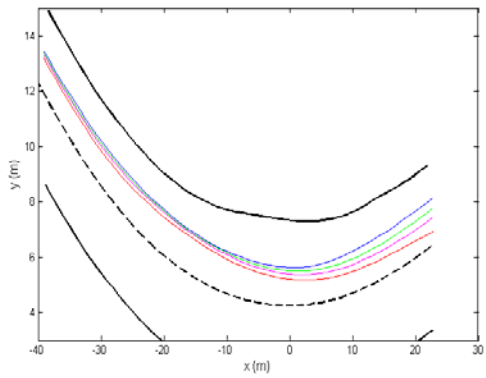

Figure 6. Reference trajectory for each driver class (not to scale).

where d_{lat} expresses the lateral distance between the reference trajectory and the simulated one, and $(\beta_n = \beta(t_n), n \in [1, N])$ the searched steer angle. There exists a different β for each speed profile due to the variation of the slip angle. The equation (9) is solved using a Newton-Raphson method.

RISK ASSESSMENT

Once the initial conditions known and the adequate reference trajectory defined, the last part of this work consists in the evaluation of a risk index, through the stochastic modeling proposed previously. The chosen risk indicator is the failure probability noted P_f, evaluated by a Monte-Carlo method [8]. While requiring a great number of simulations for accurate results, the advantage of this indicator is that it constitutes a reference solution for stochastic problems.

Probabilistic method

<u>**General principle**</u> – Let (Ω, F, P) be a probability space, where Ω is a sample space, F a σ-algebra on Ω and P a probability measure on F. The uncertain parameters of the mechanical model are gathered on a n-dimensional vector modeled as a continuous $\Re^n$-valued random variable $\boldsymbol{X} = (X_1, \ldots, X_n)^T$ defined on (Ω, F, P) whose probability density function (pdf) p_X is assumed to be known. We denote by G the limit-state function associated with the safety criterion chosen for the study. It's a measurable mapping from $\Re^n$ into $\Re$ which defines two complementary subsets of $\Re^n$: D_s and D_f, such that:

$$D_S = \{\boldsymbol{x} \in \Re^n : G(\boldsymbol{x}) > 0\} \quad (10)$$
$$D_f = \{\boldsymbol{x} \in \Re^n : G(\boldsymbol{x}) \le 0\} \quad (11)$$

called respectively the safety domain and the failure domain.
Two events are associated with these domains : the safety event $E_s \in F$ and the failure event $E_f \in F$, such that

$$E_S = \{\omega \in \Omega : G(\boldsymbol{X}(\omega)) > 0\} \quad (12)$$
$$E_f = \{\omega \in \Omega : G(\boldsymbol{X}(\omega)) \le 0\} \quad (13)$$

and which verify :

$$E_S \cup E_f = \Omega \text{ , } E_S \cap E_f = \Phi \quad (14)$$

The objective of the reliability analysis is then to evaluate the probability $P(E_s)$ or $P(E_f)$, called safety and failure probability respectively, given by :

$$P(E_s) = \int_{\Re^n} 1_{D_s}(\boldsymbol{x}) p_X(\boldsymbol{x}) d\boldsymbol{x} \quad (15)$$
$$P(E_f) = \int_{\Re^n} 1_{D_f}(\boldsymbol{x}) p_X(\boldsymbol{x}) d\boldsymbol{x} \quad (16)$$

and such that, according to Equation (14) :

$$P(E_s) = 1 - P(E_f) \quad (17)$$

where $\boldsymbol{x} = (x_1, \ldots, x_n)^T$, $d\boldsymbol{x} = dx_1 \ldots dx_n$ and 1_A (with $A = D_s$ or $A = D_f$) is the indicator function of $A \subset \Re^n$, such that : $1_A(\boldsymbol{x}) = 1$ if $\boldsymbol{x} \in A$ and $1_A(\boldsymbol{x}) = 0$ if $\boldsymbol{x} \notin A$.
Owing to Equation (17), generally only $P_f = P(E_f)$ is considered. In practice an exact calculation of P_f is not possible and a Monte-Carlo procedure must be used.

Application to the studied case – Let us recall that the vector $\boldsymbol{x}$ gathers the four parameters M, a_r, D_0, V_0 and that $\boldsymbol{X}$ is its probabilistic model. Each of its components $\boldsymbol{X_i}$ follows a truncated Gaussian distribution whose characteristics are given in Table 1. The solution $\boldsymbol{x_s}$ depends on $\boldsymbol{x}$ through the mechanical model and consequently, from Equations (7) and (8), so do the control variables $a_y(t)$ and $d(t)$. Therefore we can formally write $d(t) = d(t, \boldsymbol{x})$, $a_y(t) = a_y(t, \boldsymbol{x})$ and the safety criteria can be rewritten :

$$\overline{d} - \sup_{t \in [0,T]} |d(t, \boldsymbol{x})| > 0 \quad (18)$$
$$\overline{a_y} - \sup_{t \in [0,T]} |a_y(t, \boldsymbol{x})| > 0 \quad (19)$$

From these criteria we can define the associated limit-state functions :

$$G^D(\boldsymbol{x}) = \overline{d} - \sup_{t \in [0,T]} |d(t, \boldsymbol{x})| \quad (20)$$
$$G^A(\boldsymbol{x}) = \overline{a_y} - \sup_{t \in [0,T]} |a_y(t, \boldsymbol{x})| \quad (21)$$

and the corresponding failure events :

$$E_f^D = \{\omega \in \Omega : G^D(\boldsymbol{X}(\omega)) \le 0\} \quad (22)$$
$$E_f^A = \{\omega \in \Omega : G^A(\boldsymbol{X}(\omega)) \le 0\} \quad (23)$$

The aim of this study is then the computation of the occurrence probabilities of these failure events, given by :

$$P_f^A = P(E_f^A) \text{ , } P_f^D = P(E_f^D) \quad (24)$$

Numerical application

A set of $N = 10^7$ simulations is needed to obtain accurate probability estimations for $P_f \approx 10^{-4}$. With the specific vehicle dynamics model, the operation requires less than 2 hours on a standard PC (2GHz). The probabilities to violate the lateral acceleration criterion P_f^A and the lateral position criterion P_f^D are computed for each driver class and for speed varying from 45 to 80 km.h^{-1} (Figures 7-9).

Figure 7 shows that P_f^A vary suddenly from 0 to 1 around 60 km.h^{-1}. The driver class seems to have little influence on the probability, except for the first one that corresponds to the most interior position. Due to the fact that the curvature radius is slightly smaller, the criteria is violated at a lower speed. This first result indicates that the lateral acceleration criterion is weakly sensitive to hazard. Indeed, the speed for which P_f^A changes from 0

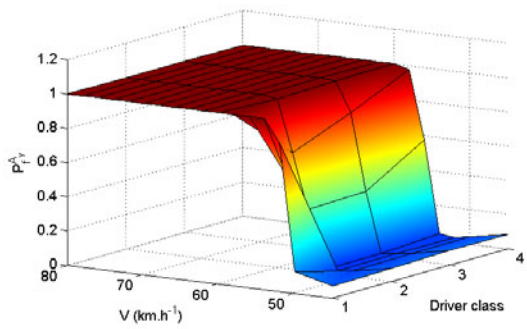

Figure 7. P_f^A as a function of speed and driver class (linear scale).

to 1 corresponds to the one that leads to reach the threshold of 3 m.s^{-2} on the different reference trajectories. This means that no information are added on this criterion compared to a deterministic study. On the contrary, Figures 8 and 9 reveal the usefulness of this probabilistic approach.

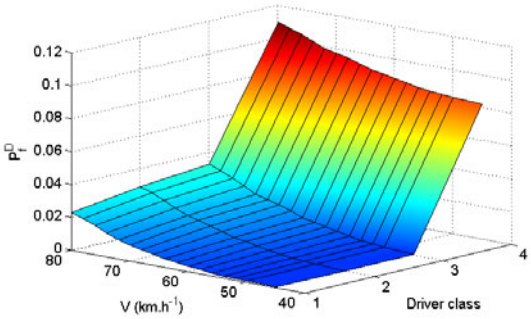

Figure 8. P_f^D as a function of speed and driver class (linear scale).

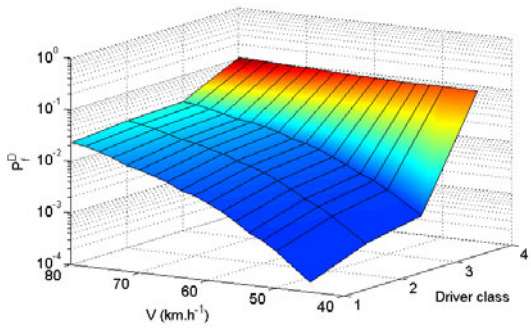

Figure 9. P_f^D as a function of speed and driver class (logarithmic scale).

Evolutions of P_f^D as a function of the speed and driver class are visible on Figure 8 (in linear scale) and on Figure 9 (in logarithmic scale). It reveals that both speed and driver class have influence on the lateral position criterion. P_f^D ranges from 10^{-4} to 0,11. The probability is always rising with increasing speed, and with the class number. This probabilistic study allows to obtain a gradation of the roadway departure risk versus speed for each driver class. This result, which could not be brought by a deterministic study, is of first interest here given the aim to trigger warning signals.

The smooth variation of P_f^D for the first three classes reveals the importance of hazard in the system. Concerning the fourth class, the probability is almost constant for all speed. This is due to the fact that it corresponds to the most exterior lane positioning (starting at only 60cm of the lane boundary) while the first class remains roughly in the middle of the lane.

In order to control a warning device, an acceptable roadway departure risk must be chosen by road safety experts considering for example real traffic analysis. Then, once a threshold on P_f^D is defined, the results of this study can be exploited to identify the critical initial conditions leading to risky situations.

CONCLUSION

This study proposes an application of probabilistic methods to the road safety domain with a view to develop a SVRD warning system. The interest of this approach is clearly highlighted for the case of an alarm triggering decision, as it leads to the direct computation of a risk indicator. This constitutes the first important difference compared to other SVRD studies. The other originality relies on the in-pavement integrated measurement devices that will be used for the initial conditions determination. This ensures a minimization of the necessary on-board equipment, which is an advantage for a mass implementation.

The results presented here show that both lateral position and speed have a great influence on the roadway departure risk. Even though these contributory factors were already well-known, the risk indicator computation allows to quantify the combined effects of these two factors. This can hardly be done with statistical post-accident analysis. Hence it has been noticed that the lateral acceleration criterion is weakly sensitive to hazard, due to the paramount influence of speed. Inversely, the lateral position criterion presents a smooth variation of probability between 10^{-4} and 0,11. Once a threshold on P_f^D is defined, the acceptable initial conditions can be selected through the results of this study. In the case where the arriving vehicle

does not respect these initial conditions, an alarm must be triggered to notify the driver to change his trajectory.

Concerning the system implementation, combined speed and lateral position measurement devices integrated in the pavement are under experimental validation. The equipped curve is the one presented in this study. The envisaged alarm system consists in warning lights positioned on the curve announcement traffic sign.

Two steps are considered for the prospects of this work. First, in the line with the driver/vehicle/road infrastructure stochastic modeling, time dependant perturbations will be added to the reference steer angle to represents the difference between the trajectory that the driver is willing to realize, and the one actually done. This involves the notion of stochastic processes, and thus requires more complex simulation and resolution methods. The statistical characteristics of this random process can be identified from experimental data and driver's actions studies. Second, a calculation time reduction will be obtained using different risk indicators and efficient structural reliability methods.

ACKNOWLEDGMENTS

This work is supported by the "Agence Nationale de la Recherche" through the project CISSSI reference ANR-06-CIS6-003.

REFERENCES

[1] G. Rey and al., "Towards a probabilistic alert procedure of roadway departure", Proceedings of the IEEE SSCI 2009 (Nashville, TN, March 30-April 2)
[2] D. Leblanc and al., "Road departure crash warning system field operational test: methodology and results", UMTRI, Tech. Rep., 2006
[3] P.H. Batavia, "Driver-adaptative lane departure warning systems", CMU, 1999
[4] D. Pomerleau and al., "Runn-off-road collision avoidance using IVHS countermeasures', NHTSA, 1999
[5] Y. Zhou and al., "A lane departure warning system based on virtual lane boundary", Journal of Information Science and Engineering 24, pp.293-305, 2008
[6] T. Piluti and A. Ulsoy, "Fuzzy-logic-based virtual rumble strip for road departure warning systems", IEEE Transactions on Intelligent Transportation Systems 4, pp.1-12, 2003
[7] A. Eidehall and L. Petersson, "Statistical threat assessment for general road scenes using monte carlo sampling", IEEE Transactions on Intelligent Transportation Systems 9, pp.137-147, 2006
[8] O. Ditlevsen and H. Madsen, "Structural Reliability Methods", Wiley, 1996
[9] A. Saltelli, K. Chan and E. Scott, "Sensitivity analysis", Wiley, 2004
[10] I. Sobol', "Global sensitivity indices for nonlinear mathematical models and their Monte-Carlo estimates", Mathematics and Computers in Simulation 55, pp.271-280, 2001
[11] J.P. Brossard, "Dynamique du véhicule : modélisation des systèmes complexes", Presses polytechniques et universitaires romandes, 2006
[12] T.D. Gillepsie, "Fundamentals of Vehicle Dynamics", Warrendale SAE, 2002
[13] H.B. Pacejka, "Tyre and Vehicle Dynamics", Warrendale SAE, 2002
[14] H. Radt and W. Milliken, "Non-dimensionalizing tyre data for vehicle simulation", Road Vehicle Handling, Institute of Mechanical Engineers, 1983
[15] D. Lechner and al., "Méthodologie de validation du logiciel de dynamique automobile CALLAS", Ingénieurs de l'automobile 713, pp.42-48, 1997
[16] J. Lauffenburger and al., "Driver-aid system using path-planning for lateral vehicle control", Control Engineering Practice 11, pp.217-231, 2003
[17] L.K. Chen and A.G. Ulsoy, "Identification of a driver steering model, and model unvertainty, from driving simulator data", Journal of Dynamic Systems, Measurement, and Control 123, pp.623-629, 2001
[18] M. Gabibulayev, "A stochastic form of a human driver steering dynamics model", Journal of Dynamic Systems, Measurement, and Control 129, pp.322-336, 2007
[19] J. Edelmann and al., "A passenger car driver model for higher lateral accelerations", Vehicle System Dynamics 45, pp.1117-1129, 2007
[20] Y. Goyat and al., "Vehicle trajectories evaluation by static video sensors", 9th International IEEE Conference on Intelligent Transportation Systems, Sept 2006